Electronic Supplementary Material (ESI) for Sustainable Energy & Fuels.

Electronic Supplementary Information

Biomimetic material polydopamine with redox-active for oxygen-promoted H_2 production from aqueous formaldehyde reforming

Leilei Du,[a] Gang Wang,[a] Xiaoqing Yan,[c] Hisayoshi Kobayashi,[d] Sha Li,[e] Renhong Li[a,b]* and Wenxing Chen[a]

a. National Engineering Lab for Textile Fiber Materials and Processing Technology, Zhejiang Sci-Tech University, Hangzhou, 310018, China. E-mail: lirenhong@zstu.edu.cn

b. Shaoxing Keqiao Research Institute of Zhejiang Sci-Tech University, Shaoxing, 312030, China.

c. Department of Chemistry, College of Science, Zhejiang Sci-Tech University, Hangzhou 310018, China.

d. Emeritus Professor of Department of Chemistry and Materials Technology, Kyoto Institute of Technology, Matsugasaki, Sakyo-ku, 606-8585, Kyoto, Japan.

e. Key Laboratory of Chemical Utilization of Forestry Biomass of Zhejiang Province, Zhejiang A & F University, Hangzhou, 311300, PR China.

Experimental

1. Synthesis of Materials

1.1 Polydopamine nanoparticles

Polydopamine nanoparticles are synthesized through oxidative polymerization of dopamine. Typically, dopamine hydrochloride (2 mg/mL) is dissolved in Tris-base buffer solution (10 mM, pH = 8.5). The solution is stirred for 12 h, and oxidation of dopamine is achieved by saturated O_2 in solution. Then the obtained dark suspension is centrifuged to collect the sediment. The sediment is washed several times with fresh water to remove unreacted dopamine, and it is then dried at 60 °C. The obtained dried sample is the PDA nanoparticles we used in this study. Then, by adjusting the drying temperature (40, 60, 90, 120, 150 and 180 °C) and obtained the PDA NPs with different degree of quinone.

1.2 Dopamine oxidation polymerization on the CF

A carbon fiber chip of 1 cm × 1 cm is cut and cleaned by ultrasonic radiation for 30 min in HNO_3 and dried in an oven before use. Dopamine solution is prepared by dissolving dopamine hydrochloride in Tris-base buffer (10 mM, pH = 8.5). The treated CF were then immersed in the above solution at 25 °C for 12 h. After that, polydopamine coated CF are ultrasonically washed with double distilled water, and then the PDA coated CF are placed in a drying cabinet.

2. Characterization

SEM images are recorded on a Zeiss Sigma 300 operated at 100 kV. Wide-angle XRD patterns are recorded on a Bruker D8 diffractometer using Cu Kα radiation. XPS is performed in a Thermo Scientific K-Alpha spectrometer. All binding energies are referenced to the C 1s peak at 284.8 eV of the surface adventitious carbon to correct the shift caused by charge effect. ^1H liquid state NMR spectrum is recorded with a Bruker Ascend 400 (400 MHz) and Bruker Avance III HD 400M spectrometer by using adamantane (δ = 38.5 ppm) as an internal standard. The samples are analyzed by FT-IR spectroscopy, using a Thermo Fisher iS10 spectrometer. Spectra are recorded in the range of wave numbers from 4000 to 400 cm^{-1}, using sample/KBr pellets prepared as described elsewhere. UV-vis absorption spectrum is recorded on a Lambda 750 UV-

vis-NIR spectrometer (PerkinElmer) equipped with an integrating sphere. The UV-vis DRS of solid samples are collected in the wavelength range of 200~800 nm against a $BaSO_4$ reflectance standard. Thermogravimetry analysis (TG) is conducted on a Netzsch TG209 F1 thermal analyzer, with a heating rate of 20 °C/min from 30 to 800 °C under a nitrogen atmosphere at a flow rate of 60 mL/min. The instrument calibration included the balance correction and temperature correction, and the temperature is reproducible to ± 0.1 °C and the mass to ± 0.1%.

X-band EPR signals are recorded on a Bruker EPR A-300 spectrometer. The settings for the EPR spectrometer are as follows: center field, 3511.39 G; sweep width, 100 G; microwave frequency, 9.86 G; modulation frequency, 100 kHz; power, 101 mW; conversion time, 10 ms. The solid EPR analysis is carried out by packing sample powders into a glass capillary tube, which is placed in the EPR chamber for testing. The location and the intensity of the g factors are determined by Bruker's WINEPR program based on $h\nu = g\beta H$, where h is Planck's constant, H is the applied magnetic field, and β is the Bohr magneton.

3. Catalytic dehydrogenation of formaldehyde solution experiments

Catalytic H_2 production from HCHO/H_2O solution is carried out with 20 mg of catalysts suspended in 5 mL of aqueous HCHO solution (1.0 M) in a 55 mL Pyrex test tube under stirring (400±10 rpm). A water bath is used to maintain the reaction temperature at 70 ± 0.5 °C. The mixture is degassed by bubbling with pure N_2 gas, and the tubes are finally sealed with silica gel stoppers. Gas volumes of 400 μL are extracted from the test tubes using a microliter syringe at regular intervals, and GC-TCD is employed for evaluating the gas evolution amount, including H_2, O_2, CO_2 and CO. TOF = $n_{H2}/(n_{PDA}\times t) \times (d/1.3)$, where n_{H2} and n_{PDA} represent the molar amounts of evolved H_2 within t h and PDA catalyst, respectively, and d is the average diameter of PDA NPs and 1.3/d is the empirical surface atom dispersion degree for nanoscale particles.

4. DFT calculations

Gaussian09 program is used throughout in his work. The hybrid B3LYP functional and 6-311G(d, p) basis set are employed. Whole reaction is supposed to proceed as (1) → (2a) → (3a) → (4) or (1) → (2b) → (3b) → (4) as shown in Scheme S3 below.

Except for (3a) and (4), there is a transition state (TS). (3a) and (4) are found to be the up-hill and down-hill reactions, respectively, without TS. For reactions with TS, the TS is characterized first, and then the intrinsic reaction coordinate (IRC) analysis is carried out for both directions, reactant and product sides. At the end point of IRC analysis, ordinary optimization run followed, and the reactant and product are optimized as the local minima.

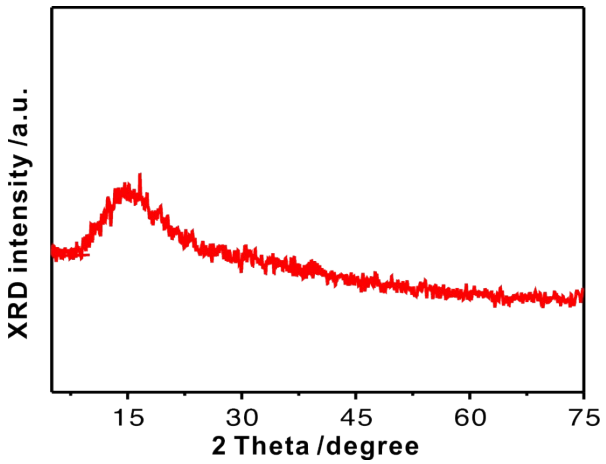

Fig. S1 XRD pattern of PDA NPs.

As shown in XRD pattern, a broad diffraction peak at $2\theta = 15^{o}$ appeared is indicate the amorphous structure and no undesirable byproducts are formed.[1]

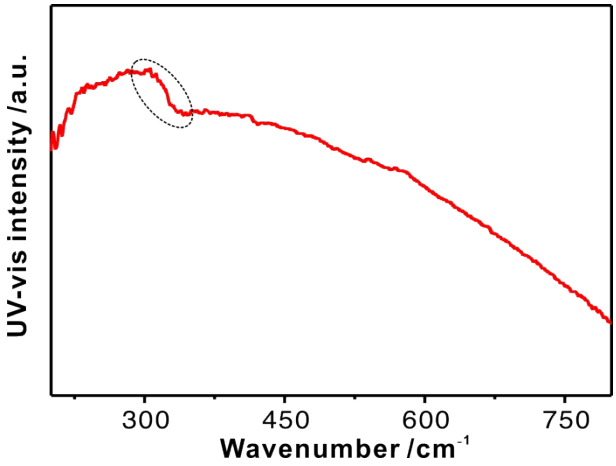

Fig. S2 UV-vis absorption spectrum of PDA NPs.

Fig. S2 has a broad-band UV−vis absorption at 320 nm relates to heterogeneity or chemical disorder of polydopamine, which is caused by the complexity of oxidative self-polymerization of dopamine.[2]

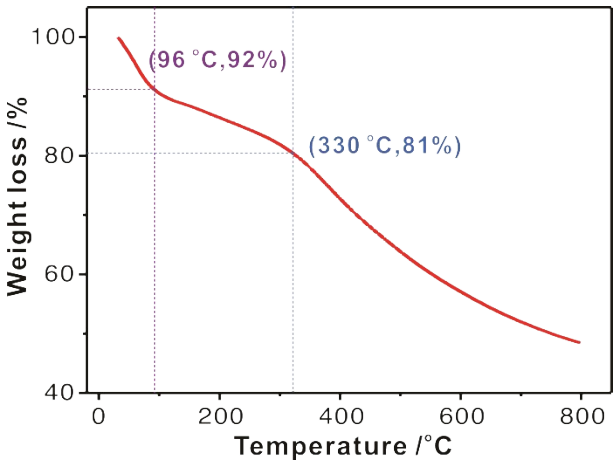

Fig. S3 TG curve of PDA NPs.

As shown in Fig. S3, based on the rate of weight loss, the TGA curve can be divided into three parts of <100 °C, 100~330 °C, and >330 °C, respectively, which corresponds to the different changing process. When the temperature is lower than 100 °C, the mass change comes from the loss of water. During the temperature range of 100~330 °C, the weight loss is due to the cross-linking of the polymer chains and conversion of the functional groups. When the temperature is increased to higher than 330 °C, carbonization proceeds, leading to fast weight loss.

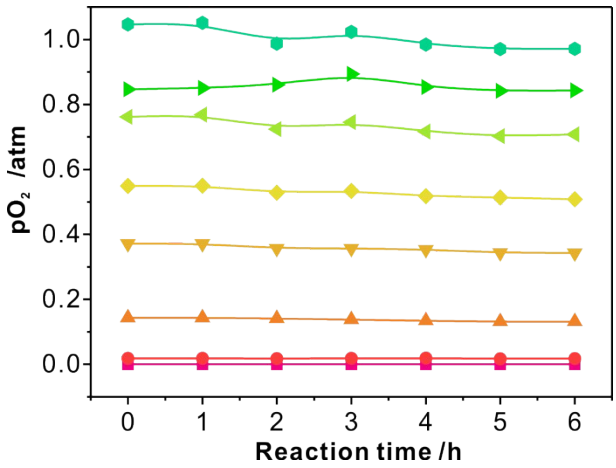

Fig. S4 The O_2 content on the H_2 evolution rate over PDA NPs in a HCHO solution as a function of reaction time.

Scheme S1 Scheme of the reaction process of the autoxidation of catechol to semiquinone and •OOH radicals.

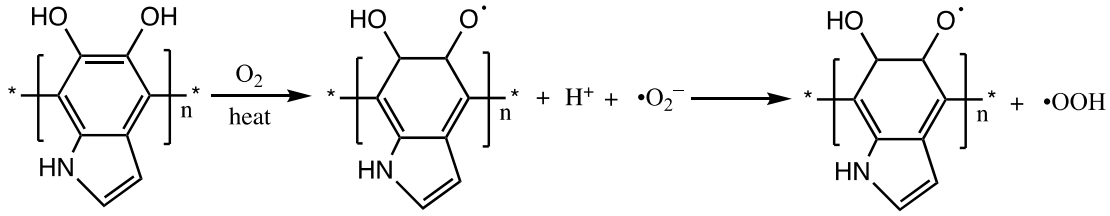

Scheme S2 Scheme of the chemical components of polydopamine after thermal treatment.

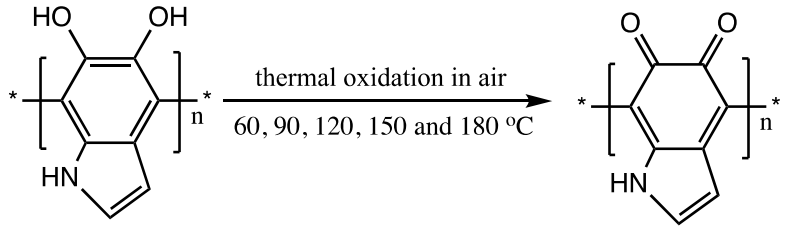

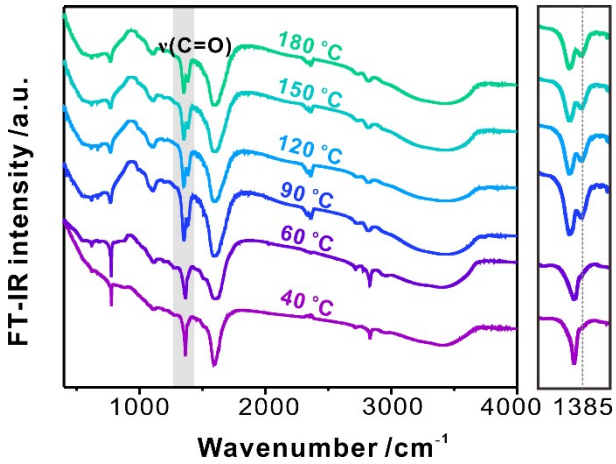

Fig. S5 The FT-IR spectroscopy of PDA NPs with different thermal treatment temperatures.

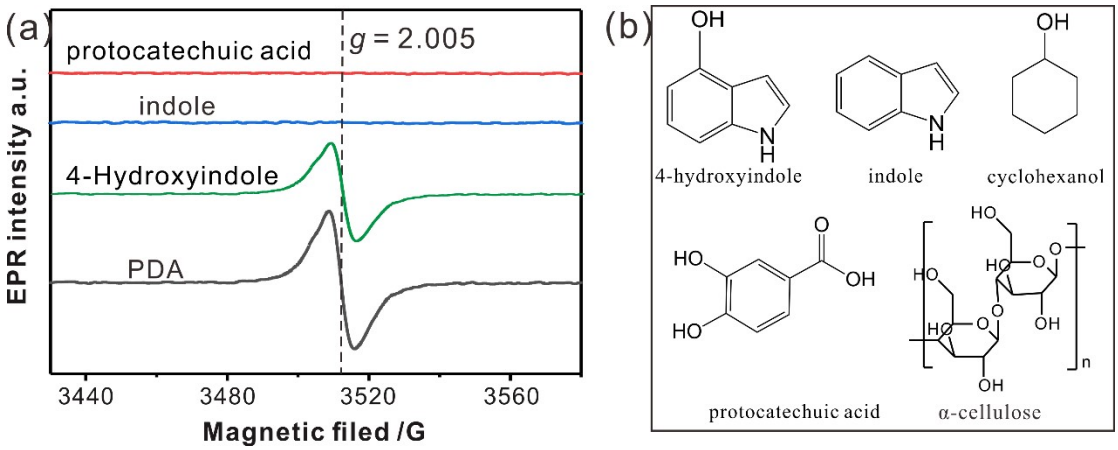

Fig. S6 (a) The solid EPR spectra and (b) chemical structural formula of 4-hydroxyindole, indole, cyclohexanol, protocatechuic acid and α-cellulose and polydopamine.

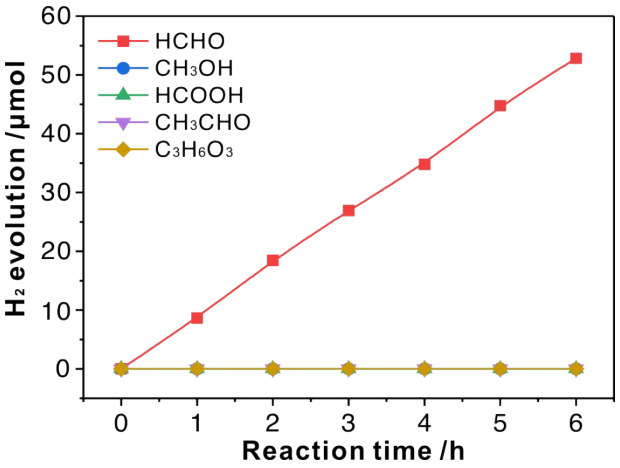

Fig. S7 The catalytic H_2 evolution from different solvents (HCHO, CH_3OH, HCOOH, CH_3CHO and $C_3H_6O_3$) over PDA NPs catalysts.

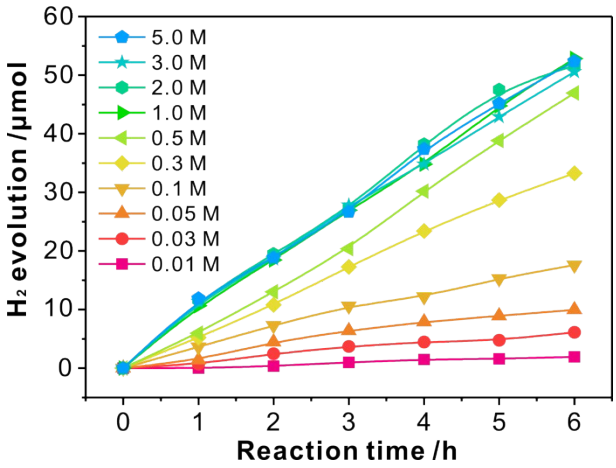

Fig. S8 The effect of formaldehyde concentration on the H_2 evolution rate over PDA NPs in a HCHO solution as a function of reaction time.

The O_2 content remains almost unaffected within 6 h of reaction irrespective of its initial concentration, indicating that O_2 has not been consumed during the entire reaction.

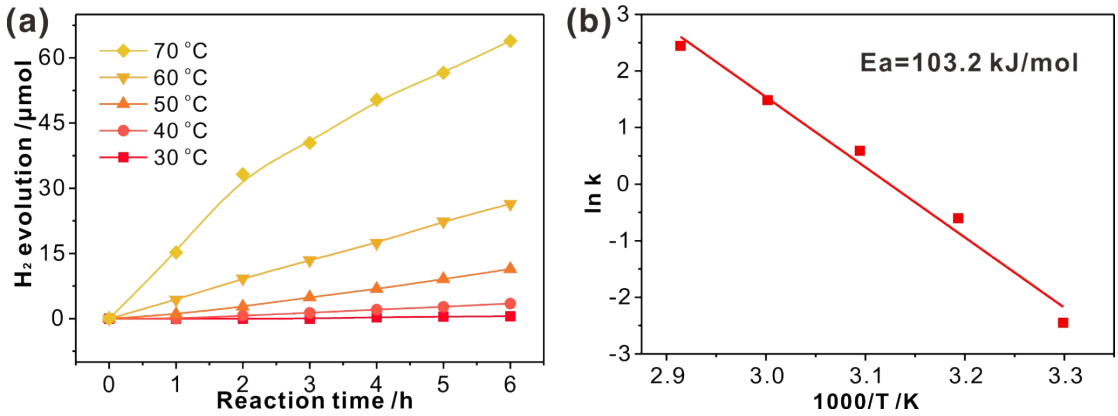

Fig. S9 (a) The effect of reaction temperature on the H_2 evolution rate over PDA NPs in a HCHO solution as a function of reaction time, and (b) corresponding Arrhenius plots.

Table S1 The elemental composition and ratios of polydopamine (theoretical value) and of prepared and reacted polydopamine coating as determined by XPS.

	C(%)	N(%)	O(%)	C/N/O
Theoretical	65.3	9.5	21.8	6.9/1/2.3
Prepared	76.7	6.9	16.4	11.1/1/2.4
Reacted	77.9	5.9	16.2	13.2/1/2.7

Table S2 The contents of different functional groups obtains by XPS high-resolution spectra fitting O1s, N 1s and C 1s of prepared and reacted PDA.

		Prepared PDA		**Reacted PDA**	
		Position /eV	Contents /%	Position /eV	Contents /%
O 1s	O−H	535.1	3.50	535.0	6.12
	C−O	532.8	78.35	533.0	66.49
	C=O	531.1	18.15	531.3	27.39
N 1s	N−H	**401.7**	**14.53**	**400.7**	**51.00**
	C−N	399.9	65.18	400.0	43.58
	C=N	**398.6**	**20.27**	**398.8**	**5.42**
C 1s	CH_x/C−NH_2	287.7	22.84	287.9	18.00
	C−O/C−N	285.8	42.61	285.9	38.82
	C=O/C=N	284.6	34.75	284.7	43.18

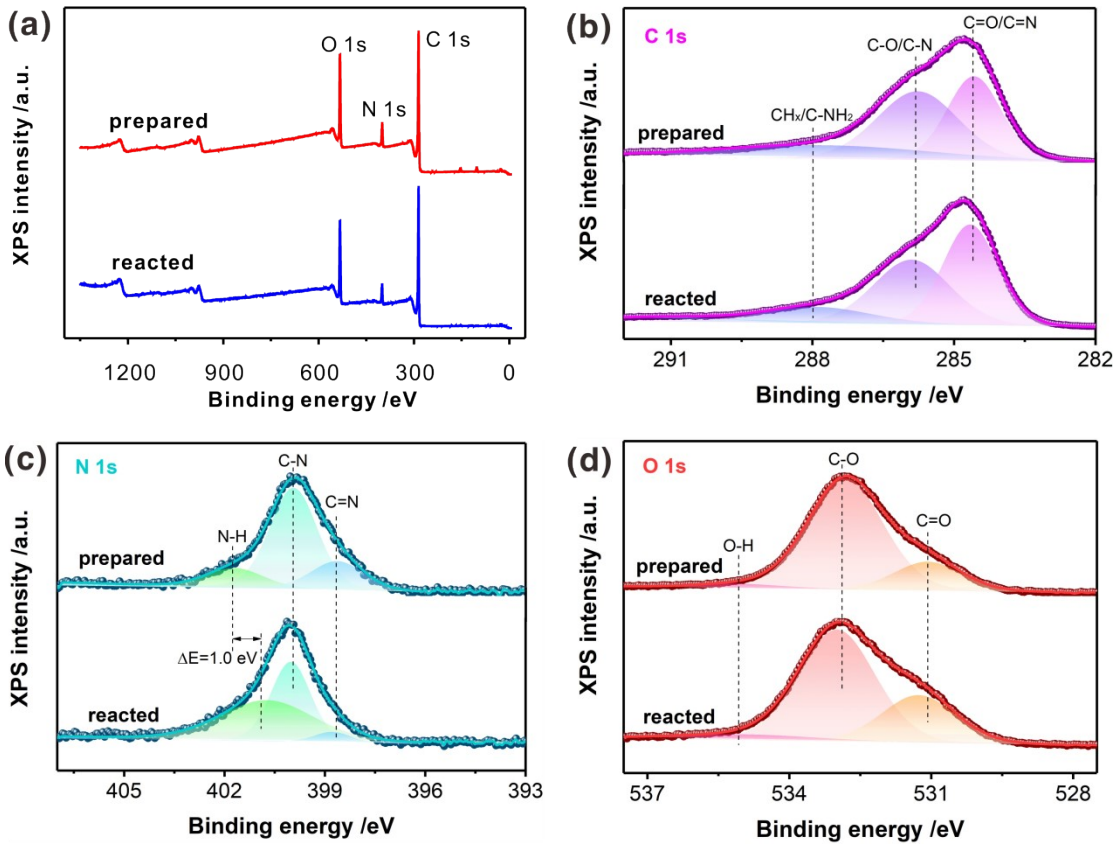

Fig. S10 (a) XPS survey spectra and high-resolution spectra of (b) C 1s, (c) N 1s and (d) O 1s regions of PDA NPs before and after catalytic reaction.

The binding styles on polydopamine surface are complicated and referring to published fitting scheme, the O 1s, N 1s and C 1s could be curve fitted into multiple main components by a best deconvolution. In comparison with the XPS spectrum of the reacted PDA with that of the pristine PDA, we can find that the N 1s peak for amino nitrogen (N−H) is shows a negative shift (ΔE=1.0 eV) and proportion increase (14.53% to 51%), while the proportion of pyridinic or aromatic nitrogen (C=N), pyrrolic nitrogen (C−N−C) decreases (65.18% to 43.58%, 20.27% to 5.42%), respectively.[3, 4] The result maybe due to the OH adsorption derive from to water molecules dissociation on the PDA.

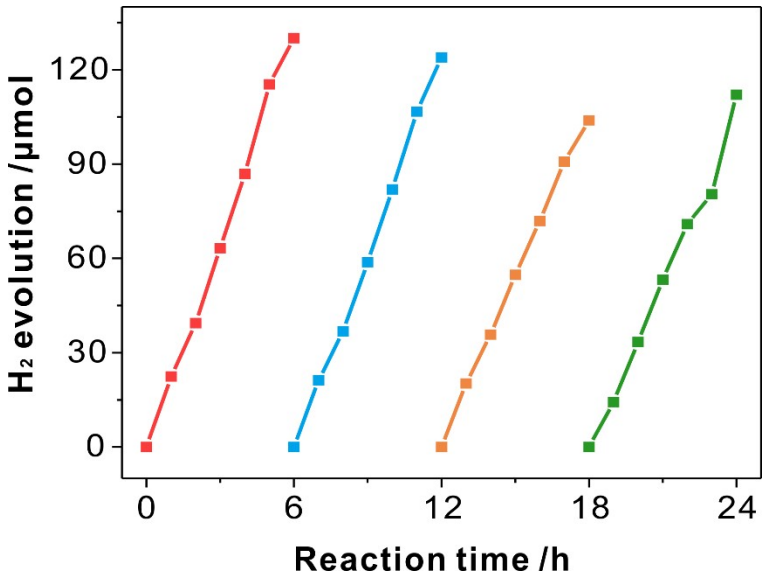

Fig. S11 The cycle performance of the PDA NPs catalyzes the hydrogen production of formaldehyde solution.

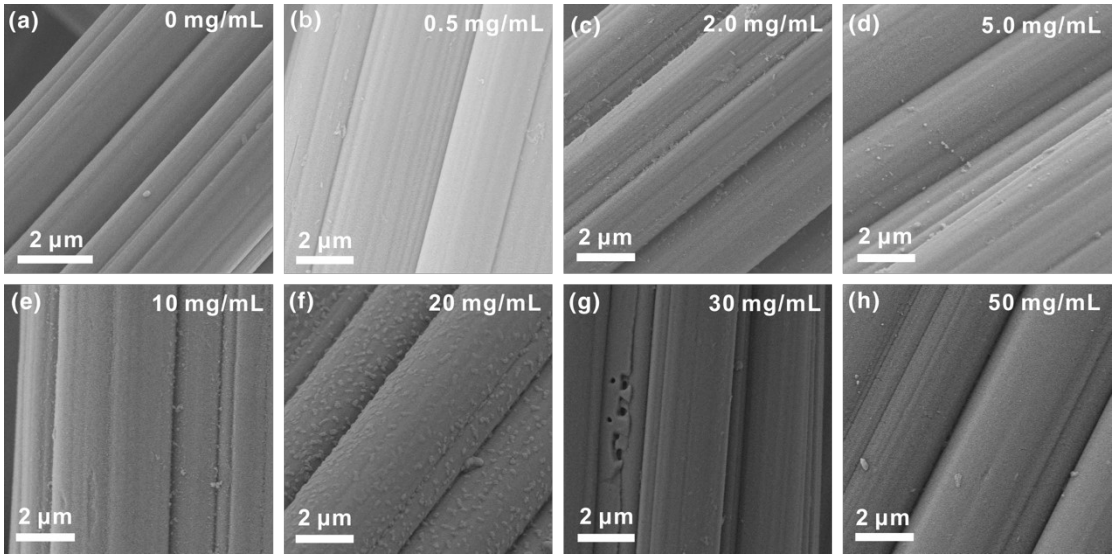

Fig. S12 The morphology of adherent ACF on the surfaces of different dopamine concentration observed by SEM.

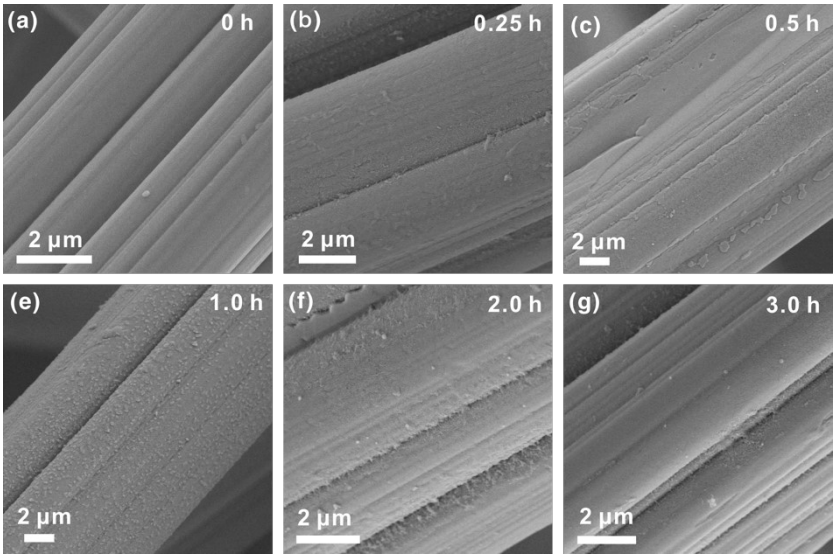

Fig. S13 The morphology of adherent ACF on the surfaces of different PDA synthesis time observed by SEM.

Table S3 Effective energy barriers and reactive sites for water dissociation and HCHO decomposition on catalysts.

Rex#	System	Total E(au)	ΔE(au)	ΔE(kcal/mol)	ΔE(kJ/mol)
#1	dopamine+O_2	-664.7578	-0.0080	-5.0	-21.0
#2	TS-1	-664.7128	0.0370	23.2	97.1
#3	dopamine(-H)+OOH	-664.7253	0.0245	15.4	64.3
#4a	HCHO+OOH	-265.4901	0.0402	25.2	105.5
#5a	TS-2a	-265.4094	0.1209	75.9	317.4
#6a	HCO+O_2+H_2	-265.4322	0.0981	61.6	257.6
#7a	dopamine(-H)+H_2O	-590.2164	-0.0132	-8.3	-34.7
	No TS				
#9a	dopamine+OH	-590.1560	0.0474	29.6	123.9
#4b	H_2O+OOH	-227.4188	0.0226	14.2	59.3
#5b	TS-2b	-227.2970	0.1444	90.6	379.1
#6b	OH+O_2+H_2	-227.3021	0.1393	87.4	365.7
#7b	dopamine(-H)+HCHO	-628.3025	-0.0104	-6.5	-27.3
#8b	TS-3b	-628.2681	0.0240	15.1	63.0
#9b	dopamine+HCO	-628.2830	0.0091	5.7	23.9
#10	OH+HCO→HCOOH	-189.8195	-0.0942	-59.1	-247.3

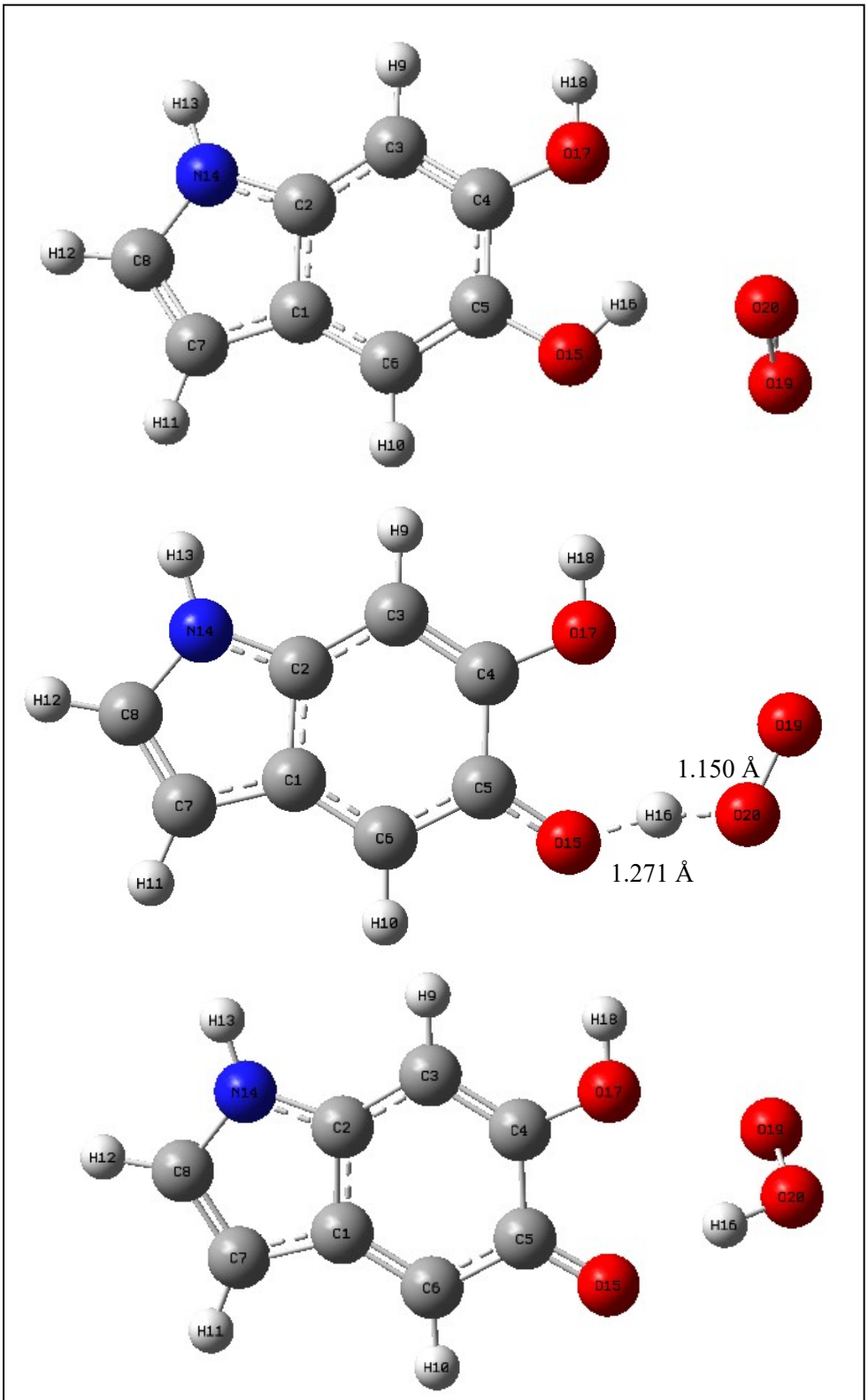

Fig. S14 Reaction (1): reactant (top), TS-1 (center) and product (bottom).

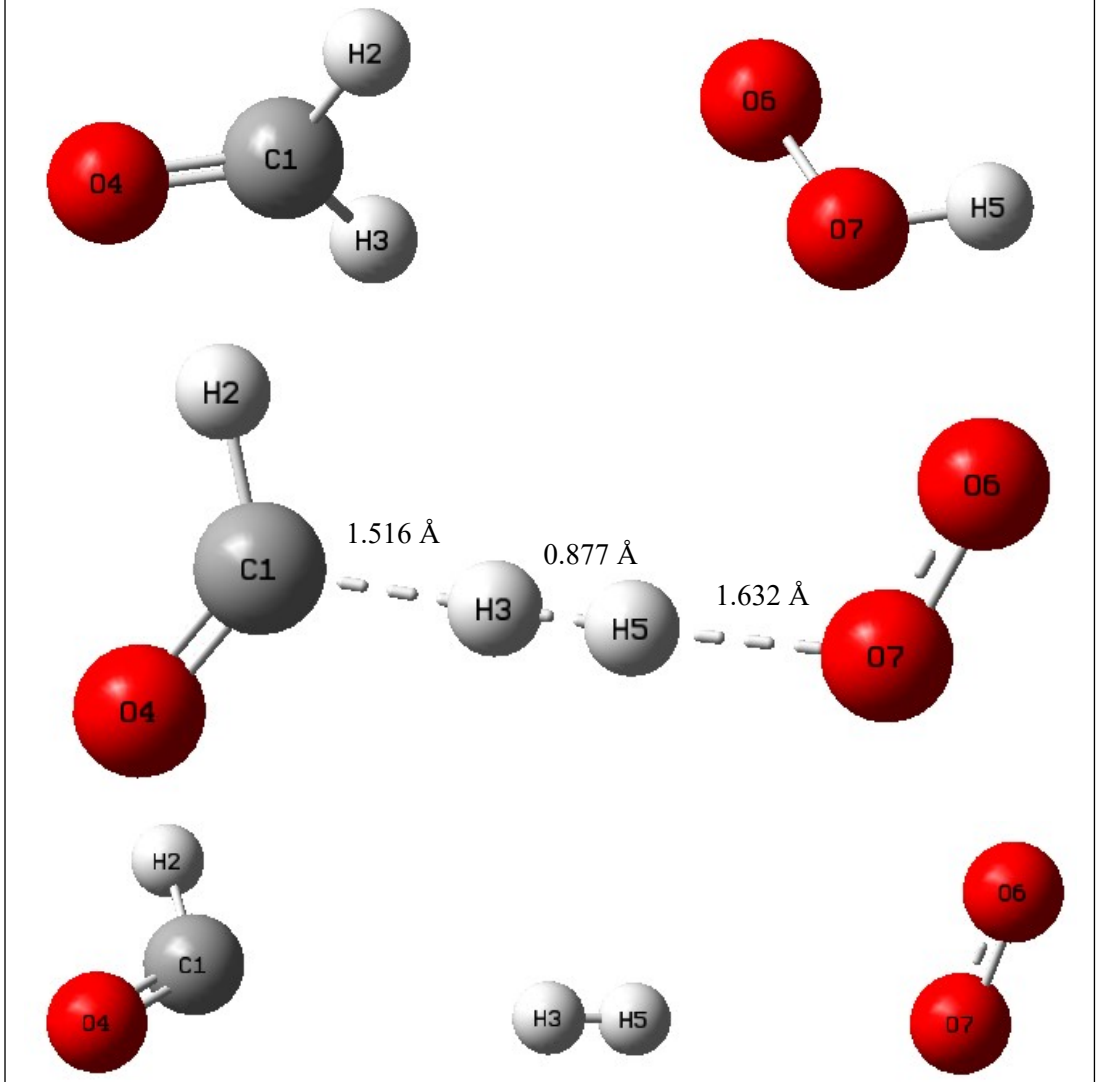

Fig. S15 Reaction (2a): reactant (top), TS-2a (center) and product (bottom).

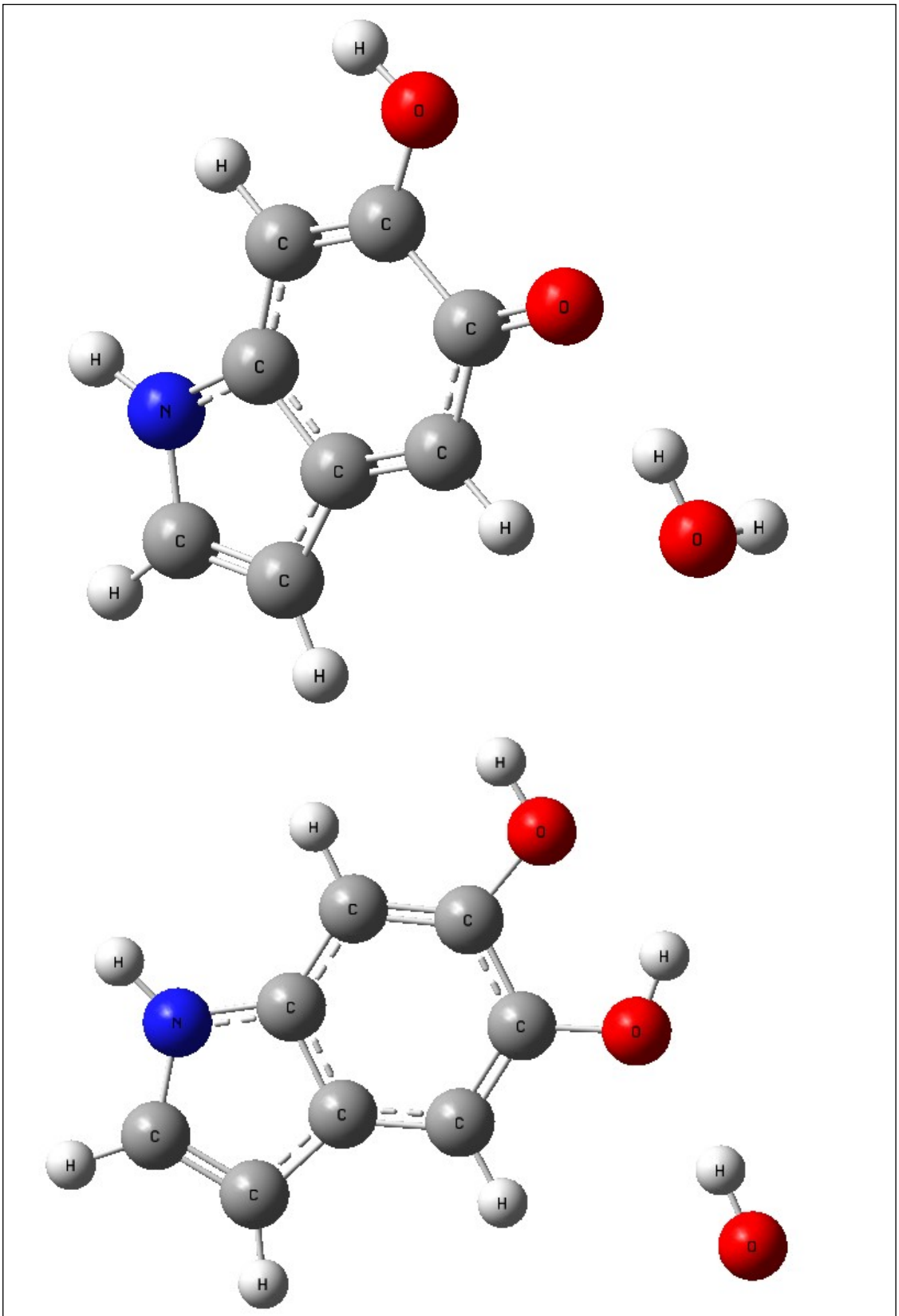

Fig. S16 Reaction (3a): reactant (top) and product (bottom). Up-hill reaction without TS.

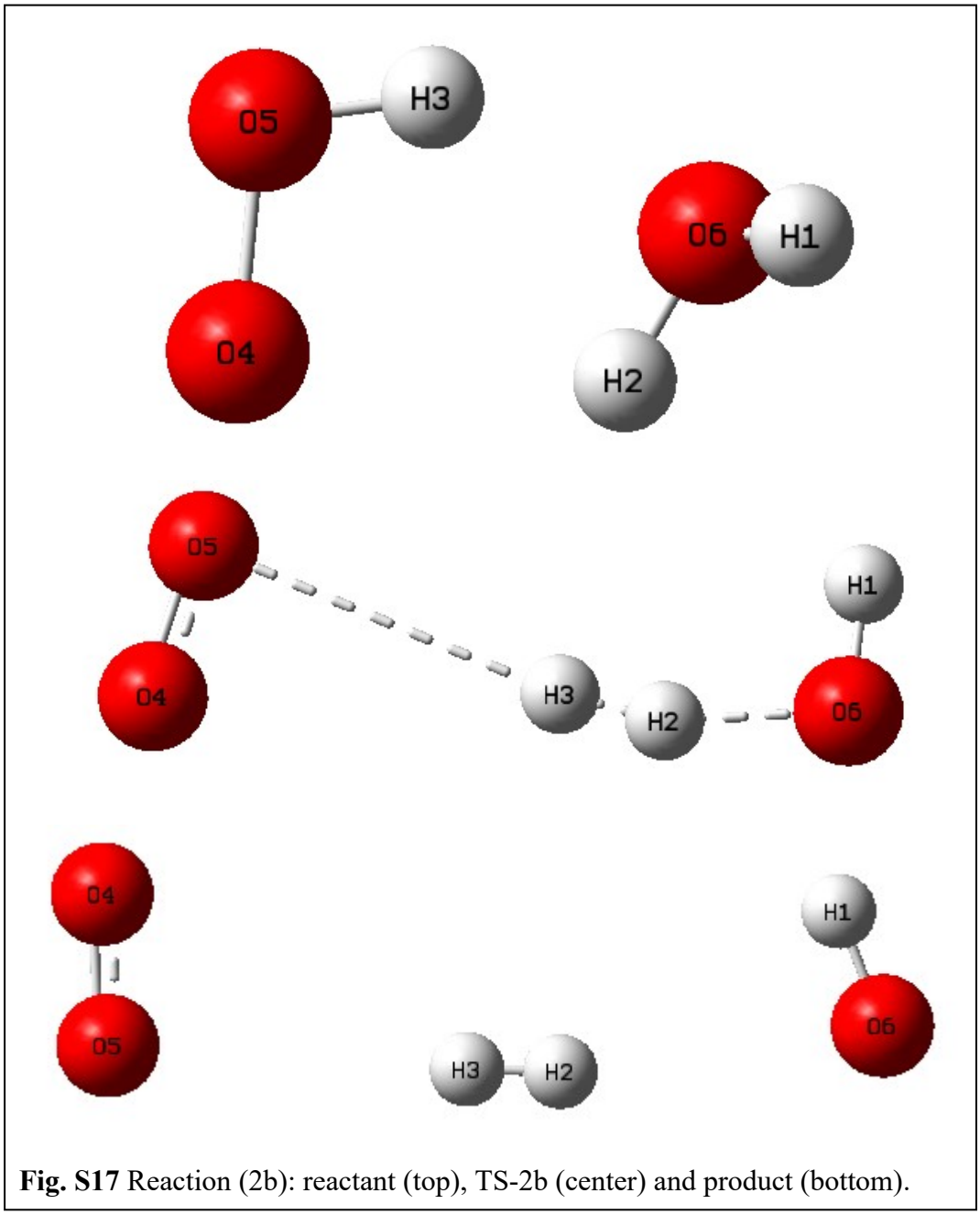

Fig. S17 Reaction (2b): reactant (top), TS-2b (center) and product (bottom).

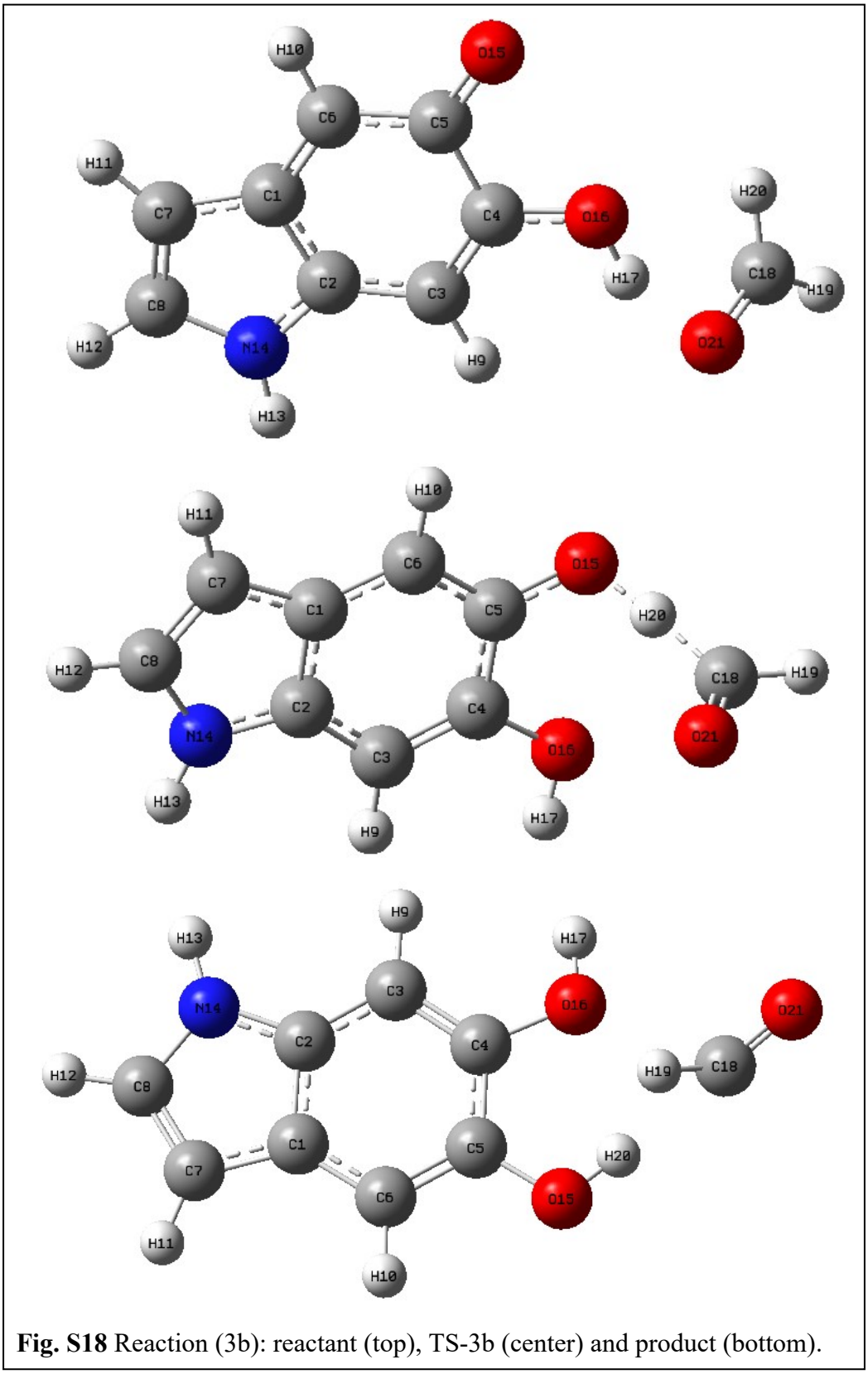

Fig. S18 Reaction (3b): reactant (top), TS-3b (center) and product (bottom).

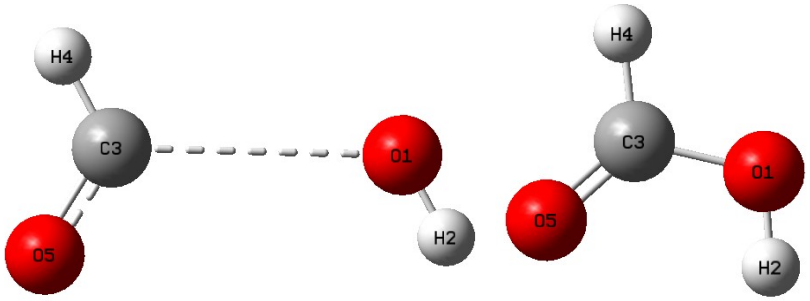

Fig. S19 Reaction (4): initial and final optimized structures.

Reference

1. H. Fan, X. Yu, Y. Liu, Z. Shi, H. Liu, Z. Nie, D. Wu and Z. Jin, *Soft Matter*, 2015, **11**, 4621-4629.
2. H. Xiang, Y. Wang, M. Wang, Y. Shao, Y. Jiao and Y. Zhu, *Nanoscale*, 2018, **10**, 13572-13580.
3. R. A. Zangmeister, T. A. Morris and M. J. Tarlov, *Langmuir*, 2013, **29**, 8619-8628.
4. Y. Zou, X. Chen, P. Yang, G. Liang, Y. Yang, Z. Gu and Y. Li, *Sci Adv*, 2020, **6**.